Available online at www.sciencedirect.com

ScienceDirect

Continental Shelf Research 27 (2007) 322–337

CONTINENTAL SHELF RESEARCH

www.elsevier.com/locate/csr

Modeling deposition by wave-supported gravity flows on the Po River prodelta: From seasonal floods to prograding clinoforms

Carl T. Friedrichs*, Malcolm E. Scully

Virginia Institute of Marine Science, School of Marine Science, College of William and Mary, Gloucester Point, VA 23062, USA

Received 4 January 2005; received in revised form 28 July 2005
Available online 9 January 2007

Abstract

A simple model for wave-supported gravity flows is applied to sediment deposition off the mouth of the Po River at time scales ranging from a single major flood to steady-state clinoform progradation. Wave-supported gravity flows are a newly appreciated class of turbidity currents, which rely on the velocity shear produced by waves near the seabed to keep sediment in suspension. The modeling approach used here, which limits the gravity flow's sediment load via a critical Richardson number, is applicable to fine sediment transport near river mouths wherever wave energy is available to move abundant sediment offshore during floods. Results suggest this phenomenon can account for the majority of the fall 2000 flood deposit mapped by EuroSTRATAFORM investigators in the vicinity of the Po River prodelta and also for the rate of prodelta progradation observed off the dominant Pila outlet of the Po over a century time-scale. Model results predict that convergence of down-slope sediment transport by wave-supported gravity flows increases with bed slope but decreases with slope gradient, such that greatest deposition occurs near where steep slopes first stop increasing with distance offshore. Thus on profiles which reach maximum steepness near shore, like those off Tolle–Gnocca–Goro mouths today or off the Pila mouth 150 y ago, gravity-driven deposition occurs in shallower water. Over time, if deposition overwhelms subsidence, the prodelta becomes less steep near shore and steeper offshore, and the locus of deposition moves progressively into deeper water. If the prodelta is prograding across a relatively flat shelf, the shape of the prodelta eventually reaches a stable form which progrades seaward as a unit. This has occurred off the Pila; but subsidence has likely overwhelmed deposition off the Tolle–Gnocca–Goro, keeping steepest slopes and maximum deposition in shallower water.

Keywords: Clinoform; Delta; Po River; Sediment transport; Turbidity currents

1. Introduction

1.1. Wave-supported gravity flows—a renewed paradigm

Observations and modeling of down-slope transport by turbid gravity flows off the Eel River in northern California associated with the Office of Naval Research (ONR) STRATAFORM project (Ogston et al., 2000; Traykovski et al., 2000; Wright et al., 2001; Scully et al., 2002, 2003; Puig et al., 2003) have reinvigorated the conceptual model of Moore (1969) that wave-supported gravity flows can play a key role in moving large quantities of mud across-shelf off of high-yield rivers. Unlike classical turbidity currents, which provide enough turbulence via their gravity-induced motion to keep

*Corresponding author. Tel.: +1 804 684 7303;
fax: +1 804 684 7250.
E-mail address: cfried@vims.edu (C.T. Friedrichs).

0278-4343/$ - see front matter
doi:10.1016/j.csr.2006.11.002

sediment in suspension, wave-supported gravity flows utilize the velocity shear associated with wave orbital velocity within the thin ($\leqslant\sim$10 cm) wave boundary layer to maintain sediment in suspension. This allows these very high concentration flows ($\sim$100 g l^{-1}) to move down-slope across much gentler slopes and over longer periods than flows associated with auto-suspending turbidity currents or with direct hyperpycnal discharge from rivers (Traykovski et al., 2000; Wright et al., 2001). As these layers move down-slope under the influence of gravity, they may deposit sediment in response to decreases in wave-induced velocity shear, bed slope or both. Another key aspect of wave-supported gravity flows is the likely role played by sediment-induced stratification in limiting the total amount of suspended sediment that wave-induced velocity shear can support. A Richardson number control of total sediment load can be derived for wave-supported gravity flows of fluid mud which predicts the sediment transport rate as a function of wave properties and bed slope, independent of other sediment or bed properties (Wright et al., 2001; Scully et al., 2002).

To test the widespread applicability of this transport mechanism, Friedrichs and Wright (2004) compared equilibrium bathymetric profiles predicted by the dynamics of wave-supported gravity flows to the bathymetry offshore of the Eel and other high-yield rivers, including the Ganges–Brahmaputra, Waiapu, Po and Rhone. They found the landward, convex-upward portion of the bathymetric profile off all these systems to be consistent with a balance between the supply of sediment by the river and the capacity of wave-supported gravity flows to move sediment offshore. This finding suggested that across-shore sediment transport associated with the formation of prodeltas (which they termed subaqueous deltas) might be dominated by wave-supported gravity flows off many rivers worldwide, even in relatively low wave energy environments like the Po. Soon afterward, the existence of wave-supported gravity flows offshore of the Po was confirmed through benthic tripod observations by Traykovski et al. (2007) as part of the ONR–European Union joint Euro-STRATAFORM Program. The purpose of the present paper is not to prove that gravity flows are solely responsible for the distribution of flood deposits off the Po, but rather to investigate whether or not wave-supported gravity flows could reasonably provide a dominant depositional mechanism during periods with appropriately favorable forcing conditions.

1.2. The PO environment

The Po, with a mean annual sediment discharge of about 13–15 million tons, drains northern Italy, including sediment from the Alps and Apennines (Nelson, 1970; Nittrouer et al., 2004; Syvitski and Kettner, 2007). Because of low tidal and remotely generated swell energy, regional winds and waves generated in the Adriatic Sea control sediment dispersal. Maximum sediment discharge typically occurs during the fall in association with increased rainfall within the drainage basin, and a secondary maximum coincides with the spring snow melt (Nelson, 1970; Syvitski and Kettner, 2007). Fine sediment discharged from the Po is highly flocculated within the river due to its relatively large organic content (Fox et al., 2004). High flocculation favors very rapid settling in the immediate vicinity of the river mouth such that, in the absence of strong waves or coastal currents, muddy deposits produced by settling of sediment from the river plume begin to form in 4 m of water, and the bulk of suspended material is removed from the water column by 6 m depth (Fox et al., 2004).

There are two main routes of Po sediment dispersal if high discharge coincides with strong winds, waves and/or currents: along-shore to the southwest in association with buoyancy, wind and wave-driven mean currents, and across-shore and down-slope in association with down-welling currents and sediment-induced gravity flows (Nittrouer et al., 2004; Sherwood et al., 2004; Traykovski et al., 2007). Although the waves off the Po are smaller and shorter period than those in open shelf environments, such as the Eel shelf off California, wave-driven processes can still dominate at times, albeit in a zone moved to comparatively shallower depths (Nittrouer et al., 2004). Because sediment settles closer to shore and waves are smaller, it follows that wave-supported gravity flows, if and when they occur, begin and end in much shallower water than that observed off the Eel.

Since the late 1800s, the major outlet of the Po has been the Pila (Fig. 1), which is estimated to discharge about 60–75% of the total Po sediment load under normal conditions (Nelson, 1970; Syvitski et al., 2005). However, it is likely that the secondary distributaries become more active during high discharge events (Wheatcroft et al., 2006).

According to Nelson (1970), the average rate of progradation of the Pila shoreline between 1860 and 1959 was about 35 m yr^{-1}. At present, the progradation rate of the Pila is closer to its pre-anthropogenic rate of about 4 m yr^{-1} (Syvitski and Kettner, 2007). In the mid-19th century, the major outlet of the Po had been the Tolle, which advanced during the mid-1800s at about 60 m yr^{-1} (Nelson, 1970). Historically, growth of the Po delta system has been characterized by alternating periods of rapid advance and abandonment of its multiple deltaic lobes, including major avulsions. Two basic types of prodelta deposits occur in high-resolution seismic records (Correggiari et al., 2005): (i) shingled lobes characterized by laterally continuous seismic reflectors consistent with preserved flood layers and (ii) prodelta lobes accompanied by massive cut-and-fill features. The latter may represent past periods dominated by direct hyperpycnal discharge from the river (Correggiari et al., 2005), whereas the former appears more consistent with present-day transport processes, including perhaps wave-supported gravity flows.

1.3. Observations of Po floods during EuroSTRATAFORM

The fall 2000 flood was one of the largest in the Po river basin within the past 100 y (Wheatcroft et al., 2006). Based on historical rating curves, up to 40 million tons of sediment may have been discharged by the Po between October and December 2000 (Syvitski and Kettner, 2007). Although EuroSTRATAFORM instrumentation was not yet in the water, a EuroSTRATAFORM event response cruise was conducted in early December 2000 to box core the resulting flood deposit (Nittrouer et al., 2004; Palinkas et al., 2005; Wheatcroft et al., 2006). Based on the depth of ^{7}Be penetration (Palinkas et al., 2005) and the physical sediment signatures

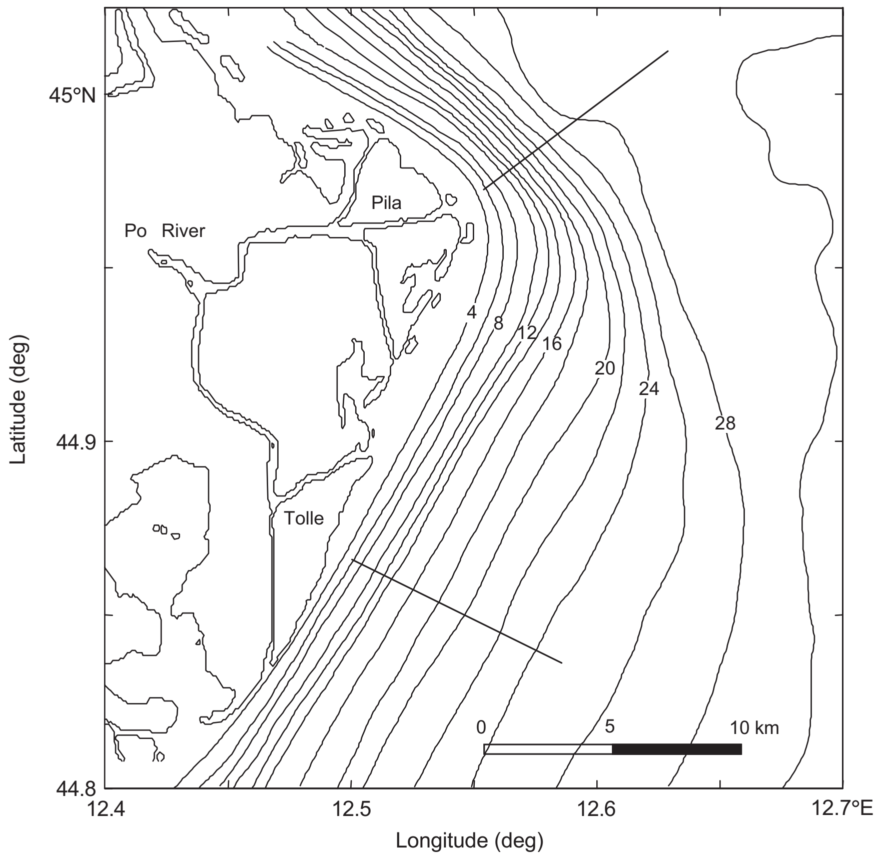

Fig. 1. Location map and bathymetry of the shelf in the immediate vicinity of the Pila, the main distributary of the Po River, Italy. Bathymetric data from Correggiari et al. (2001) provided in digital form by F. Trincardi. The profile lines indicate the portions of the prodelta offshore of the Pila and Tolle distributaries that are plotted in Fig. 8(c).

visible in X-radiographs (Wheatcroft et al., 2006), the integrated mass of the flood deposit was estimated to be about 13–16 million tons. The main depocenter exceeded 35 cm in thickness in 20 m of water off the mouth of the Pila, with a secondary depocenter reaching about 25 cm in thickness in 10 m of water off the Tolle–Gnocca–Goro distributaries (Fig. 2).

Benthic tripods deployed offshore of the Gnocca mouth in the fall and winter of 2002–2003 documented a second large flood of the Po, at which time water discharge reached about 80% of the 2000 level (Nittrouer et al., 2004; Traykovski et al., 2007). In particular, at their 12-m tripod, Traykovski et al. (2007) observed wave-supported gravity flows of fluid mud within the wave boundary layer moving down-slope at 5 cm s^{-1}. Similar to the pattern seen off the Eel, Traykovski et al. (2007) found that these sediment gravity flows off the Po were limited to periods of relatively large waves. Unlike the mid-shelf off the Eel, however, Traykovski et al. (2007) concluded that the fraction of the total sediment transport accounted for by wave-supported gravity flows at the Gnocca 12-m site over the course of the deployment was minor compared to the along-shore transport advected by mean currents. Nonetheless, it is still possible that wave-supported gravity currents may dominate transport during the largest floods of the Po, especially with regards to across-shore transport offshore of the Pila, which is the main outlet of the Po. According to Syvitski et al. (2005), sediment discharge from the Pila is typically 5–7 times greater than that from the Gnocca. Furthermore, the bed slope at 12-m is more than twice as steep off of the Pila than off the Gnocca.

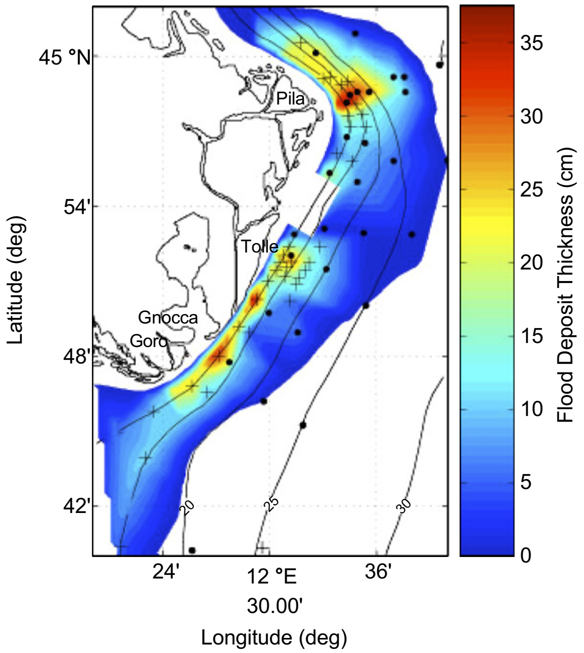

Fig. 2. Isopach map of the fall 2000 Po River flood deposit based on sampling in December 2000 (●) and October 2001 (+) from Wheatcroft et al. (2006). Also shown are the outlets of the four main distributaries of the Po. Reprinted from Wheatcroft, R.A., Stevens, A., Hunt, L.M., Lewis, R., 2006. The large-scale distribution and internal geometry of the fall 2000 Po River flood deposit: evidence from digital x-radiography. Continental Shelf Research 26, 499–516, Copyright (2006), with permission from Elsevier.

1.4. Wave-supported gravity flows and existing models for clinoform geometry

Along with the potential dominance of across-shore sediment transport during floods, wave-induced gravity flows also provide a possible mechanism for explaining the observed geometry of prodeltas and shallow clinoforms perched atop pre-existing shelves, such as that found off the Po. Pirmez et al. (1998) pointed out that the convex-upward, landward portion of a clinoform is most easily explained by a slope-dependent advective sediment transport process which decreases in intensity with greater water depth. Wave-supported gravity flows are highly consistent with this general inference. In contrast, diffusive transport approaches for generating clinoforms generally produce concave-up profiles all the way to the shoreline. A limitation in the details of the Pirmez et al. (1998) approach, however, was that the bed stress associated with maintaining the sediment load was simply set to be inverse to the water depth, and was not tied explicitly to wave energy.

A recent advancement in simple clinoform modeling by Swenson et al. (2005) ties offshore sediment advection on the shelf to the product of bed slope and a power of the wave orbital velocity, which is assumed to decay offshore in deeper water according to shallow water wave theory. The result of long-term profile simulations by Swenson et al. (2005) is then a convex upward topset–foreset component which broadens with decreased river sediment supply or with increased wave energy. This predicted trend is highly consistent with Friedrichs and Wright's (2004) analytical model for equilibrium profiles off river mouths which was based explicitly on wave-supported gravity flows. Friedrichs and

Wright (2004) found the equilibrium convex-up portion of the bathymetric profile off river mouths to be a function of wave climate and riverine sediment supply only, with deeper and broader profiles associated with decreasing sediment supply, increasing wave height and/or increasing wave period.

2. Theoretical development

2.1. Governing relations

The time-averaged, depth-integrated momentum balance for a wave-supported sediment gravity flow, within which negative buoyancy results from sediment suspension by waves, is given approximately by a balance between the down-slope pressure gradient induced by the turbid layer and opposing mean bottom stress (Fig. 3)

$$\alpha g s C \rho_s^{-1} = c_d |u| u_g. \tag{1}$$

In Eq. (1), α is the sine of the bed slope, g is the acceleration of gravity, ρ_s is the density of siliceous sediment and s is its dimensionless submerged weight relative to sea water, C is the depth-integrated mass concentration of suspended sediment within the wave boundary layer, and $c_d \approx 0.003$–0.004 is the bottom drag coefficient (Wright et al., 2001; Scully et al., 2002). (Note that α, "slope" and dh/dx, where h is depth, are all very nearly equal and will be used interchangeably for $\alpha \ll 1$). The key velocities associated with Eq. (1) are the down-slope velocity of the gravity current (u_g) and the absolute amplitude of the instantaneous velocity, $|u| \approx (u_w^2 + u_g^2)^{1/2}$, where ($u_w$) is the root-mean-square (rms) amplitude of the wave orbital velocity, all evaluated near the top of the wave boundary layer.

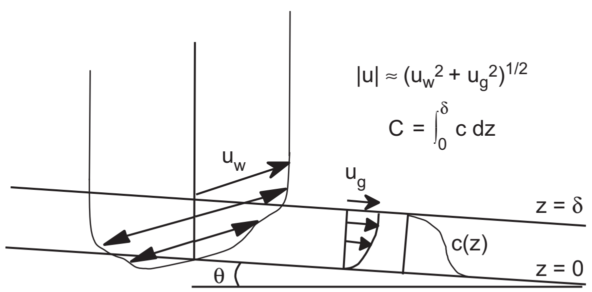

Fig. 3. Schematic diagram of a sediment-induced gravity current of depth-integrated concentration C, trapped within a wave boundary layer of thickness δ, and moving across a continental shelf of bed slope θ. The velocity scale $|u|$ accounts for the contribution to quadratic friction of both wave orbital velocity (u_w) and the speed of the gravity current (u_g).

A second key relation is the Richardson number for suspended sediment within the wave boundary layer

$$Ri = g s C \rho_s^{-1} |u|^{-2} \tag{2}$$

which compares the relative influence of buoyancy and shear on the generation of turbulence by shear instabilities within the wave boundary layer. For wave-supported gravity flows on the Eel River shelf, Wright et al. (2001) and Scully et al. (2002) showed that observed transport and deposition rates of suspended sediment could be explained by Eqs. (1) and (2) in combination with a feedback mechanism which maintains Ri in Eq. (2) near its critical value of $Ri_c = 1/4$. For $Ri < 1/4$, turbulence associated with intense shear instabilities suspends additional sediment, increasing C and Ri, while for $Ri > 1/4$, decreased generation of shear instabilities reduces turbulence and causes sediment to settle. Because the maximum sediment load is determined by the critical Richardson number, this approach for predicting sediment concentration is not dependent on detailed sediment or bed properties. The only requirements regarding the sediment are that a sufficient supply of easily suspended material be available to produce critical stratification and that its fall velocity be small enough that it stratifies the full thickness of the wave boundary layer.

2.2. Analytical solution for deposition

Combining Eqs. (1), (2) and the definition of $|u|$ then yields the following analytical solution for the maximum turbulent sediment load that a wave-supported gravity current can transport down-slope, $Q_g = u_g C$:

$$Q_g = \frac{\alpha Ri_c^2 \rho_s u_w^3}{c_d s g \{1 - (\alpha Ri_c / c_d)^2\}^{3/2}} \tag{3}$$

(Scully et al., 2002). The magnitude of down-slope sediment transport, Q_g, increases with near-bed wave orbital velocity, u_w, and bed slope, α. Thus the rate of deposition, $D = -dQ_g/dx$, will also increase with u_w and α, and further be controlled by gradients in u_w and α

$$D = Q_g \left\{ -\frac{3}{u_w}\frac{du_w}{dx} - \frac{(1+2\beta)}{\alpha(1-\beta)}\frac{d\alpha}{dx} \right\}, \tag{4}$$

where $\beta = \alpha Ri_c / c_d$.

The first term in the bracketed expression in Eq. (4) represents the drop in gravity flow transport capacity as wave orbital velocity decays offshore (toward positive x). Assuming a monotonically deepening profile, $\mathrm{d}u_\mathrm{w}/\mathrm{d}x$ is always negative, and the contribution of this first term to deposition is always positive. The second term in the bracketed expression increases deposition if the bathymetric profile is concave upward ($\mathrm{d}\alpha/\mathrm{d}x<0$) and decreases deposition if the bathymetric profile is convex ($\mathrm{d}\alpha/\mathrm{d}x>0$). Physically, $\mathrm{d}\alpha/\mathrm{d}x<0$ slows the gravity flow, increasing convergence, whereas $\mathrm{d}\alpha/\mathrm{d}x>0$ accelerates the gravity flow, decreasing convergence. Though strictly applicable only near shore and where slopes are gentle, a simplification useful for further interpreting Eq. (4) is to consider the case of shallow water waves and small β. Then Eq. (4) reduces to

$$D=\frac{\alpha Ri_\mathrm{c}^2\rho_\mathrm{s}}{c_\mathrm{d}sg}\left\{\frac{H}{2}\sqrt{gh}\right\}^3\left\{\frac{3}{2}\frac{\alpha}{h}-\frac{1}{\alpha}\frac{\mathrm{d}\alpha}{\mathrm{d}x}\right\}, \tag{5}$$

where H is rms wave height.

Eq. (5) highlights the sensitivity of deposition to both slope (α) and the slope gradient ($\mathrm{d}\alpha/\mathrm{d}x$). All else held constant, greater slope at a given location increases deposition because the down-slope sediment transport rate (Q_g) and the rate of decay of wave orbital velocity ($\mathrm{d}u_\mathrm{w}/\mathrm{d}x$) both increase with greater α, together increasing the magnitude of flux convergence. This is true for both the general case in Eq. (4) and the shallow water case in Eq. (5). If α is also increasing offshore, however, $\mathrm{d}\alpha/\mathrm{d}x$ tends to decrease deposition. On a sigmoid-shaped profile characteristic of a prodelta or clinoform, $\mathrm{d}\alpha/\mathrm{d}x$ eventually changes sign, and α begins to decrease with greater x. This slope maximum is the point where the positive effect of α on deposition is greatest and the negative effect of $\mathrm{d}\alpha/\mathrm{d}x$ on deposition has disappeared. Thus, this is the region of maximum deposition. Although a switch to $\mathrm{d}\alpha/\mathrm{d}x<0$ further favors deposition via its effect on the second bracketed term in Eqs. (4) and (5), $\mathrm{d}\alpha/\mathrm{d}x<0$ eventually reduces deposition farther offshore because α (and the magnitudes of Q_g and $\mathrm{d}u_\mathrm{w}/\mathrm{d}x$) must also be decreasing. To put it all together conceptually, along a bathymetric profile dominated by wave-supported gravity flows, the maximum rate of sediment flux convergence and associated deposition tends to be near where the slope of the bed first stops increasing with depth offshore.

2.3. *Control of wave-supported gravity flows by sediment supply and wave-base*

The above solution for deposition assumes that the available supply of riverine sediment exceeds the local capacity for down-slope sediment flux. Otherwise, sediment flux will be limited by the available sediment supply, not by Q_g, and there will be no convergence in gravity-driven transport. Very close to shore in very shallow water, even relatively small waves are associated with large u_w and will have a large capacity to maintain sediment in suspension via the Richardson number criterion in Eq. (2). Thus, deposition associated with wave-supported gravity flows during floods will begin at some finite distance offshore where Q_g drops below the supply from "up-stream". And the maximum rate of deposition is expected where the slope of the bed first stops increasing beyond that point.

The exponential decay of wave orbital velocity in deep water ultimately limits the depth at which the above analysis applies. If u_w is less than about $10\,\mathrm{cm\,s^{-1}}$, it is unlikely that waves would be the dominant source of shear determining how much fine sediment would remain in suspension. Applying linear wave theory to ~2 m height, 6–7 s waves characteristic of the wave-supported gravity flows observed off the Gnocca during fall 2002 (Traykovski et al., 2007), the maximum depth one would expect wave-supported gravity flows could dominate transport would then be at a wave base of about 30 m. For longer period waves during flood-associated storms on the far more energetic Eel shelf, the maximum depth can extend past 100 m. Nonetheless, wave-supported gravity flows are likely to dominate progradation of an entire clinoform only when it is perched on top of a pre-existing shelf. This situation is relatively common with regards to prodeltas, but when entire shelves prograde seaward as clinoforms, the offshore, concave upward portion of the clinoform extending into the deep sea must be governed by other types of gravity flows.

3. Application to the Po fall 2000 flood

3.1. *Model grid and environmental forcing*

The model domain as applied here consists of a 118 by 92 element rectangular grid covering a region close to the entire area displayed in Fig. 1, with a 240 m spacing in the predominantly across-shore east–west direction and a 330 m spacing in the mainly along-shore north–south direction. The bathymetry for the model is the same bathymetric database used in plotting Fig. 1 (from Correggiari et al., 2001), interpolated onto the above grid, and then smoothed both north and south using a cubic spline on every ninth bathymetric point. Bathymetric smoothing is necessary because frictionally dominated gravity flows will otherwise pool unrealistically behind small irregularities in bathymetry. Because of complex bathymetry to the southwest of the Gnocca mouth, our model domain does not extend quite as far south as the observations of flood deposition in Fig. 2. Model bathymetry is not updated by deposition over the course of the single season simulations.

Significant wave height and period used to force the model were collected every three hours at the wave buoy located offshore of Ancona, Italy, and were obtained from L. Cavaleri (Pers. Commun.) (Fig. 4a). A partial time-series of wave heights was also available offshore of Venice, which is closer than Ancona to the Po delta. Unfortunately, there were too many gaps in the Venice time-series for it to be useful. Fig. 4(a) shows that for times that both wave sites reported data, the two time-series were remarkably similar. Because the Ancona data were much more complete, they were chosen to force the numerical model. The rms amplitude of near-bed wave orbital velocity, u_w, was calculated for each point in the model grid by interpolating the wave heights and periods observed at Ancona to each model time step and applying linear wave theory to calculate the decay of wave orbital velocity with depth. Daily river water discharge needed to estimate sediment load was measured 92 km above the river mouth at the Pontelagoscuro station for the years 1989–2003 (Syvitski and Kettner, 2007).

Sediment discharge from the Po River before separation into its distributaries was initially estimated by applying the rating curve of Syvitski et al. (2005) for a single river channel neglecting random variability:

$$Q_s/<Q_s> = f(Q_w/<Q_w>)^c, \tag{6}$$

where Q_s is daily suspended sediment discharge in $\mathrm{kg\,s^{-1}}$, Q_w is daily water discharge in $\mathrm{m^3\,s^{-1}}$, $< >$ indicates long-term averages, and f and c are empirical constant coefficients. The following values for the Po were provided by A. Kettner and

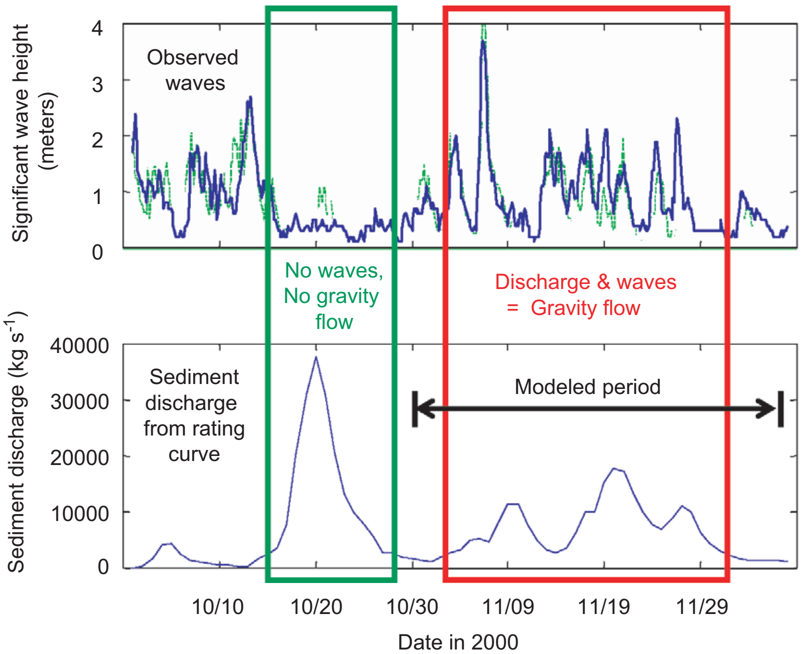

Fig. 4. (a) Significant wave height from the Ancona wave buoy (dark, solid line) and Venice wave tower (light, dashed line) provided by L. Cavaleri (pers. commun.). (b) Po suspended sediment discharge from rating curve provided by A. Kettner and J. Syvitski (pers. commun.). Boxes indicate the two main portions of flood, each highlighting times with $Q_s > 2500\,\mathrm{kg\,s^{-1}}$. The first portion has much lower waves than the second and, presumably, much weaker wave-supported gravity flows. The heavy two-headed arrow indicates the full duration of 2-D model run.

J. Syvitski (Pers. Commun.) for the period 1989–2003: $<Q_s> = 538\,\mathrm{kg\,s^{-1}}$, $<Q_w> = 1540\,\mathrm{m^3\,s^{-1}}$, $f = 0.296$ and $c = 2.98$. Fig. 4(b) displays calculated suspended sediment discharge based on Eq. (6).

3.2. Implementation of 2-D model for wave-supported gravity flows

For the region encompassing the Po prodelta, the equations governing wave-supported gravity flows were implemented in the same manner as that described for the Eel shelf by Scully et al. (2003). Basically, this numerical implementation solves Eq. (3) if there is sufficient riverine sediment load available to critically stratify the wave boundary layer according to the Richardson number criterion in Eq. (2). Local deposition is then given by the 2-D convergence of Q_g. Deposition of new flood sediment is kept track of and is available for later resuspension. If there is not enough sediment arriving from up-slope at a given location to satisfy the Richardson criteria and $|u|$ is above a specified critical velocity for resuspension from the bed, u_{cr}, material deposited at that location since the run began is added to the wave boundary layer until Eq. (2) is satisfied. If previously deposited sediment is also insufficient to satisfy Eq. (2), C is simply set to the total amount of sediment available, and Eq. (1) is used to solve for u_g. Down-slope sediment flux is then known from $Q_g = u_g C$, but no deposition occurs. Identical to Scully et al. (2003), the critical velocity for bed erosion was set to $35\,\mathrm{cm\,s^{-1}}$, the critical Richardson number was set to $Ri_c = 0.25$, and the bottom drag coefficient was set to $c_d = 0.003$. Sediment porosity for conversion to deposit thickness was set to 0.8 based on the results of Palinkas et al. (2005) and Wheatcroft et al. (2006).

Consistent with available observations of wave-supported gravity flows off both the Po and Eel Rivers, the 2-D model was applied only to the portion of the fall 2000 Po flood characterized by high wave energy (Fig. 4). This constraint is consistent with the results of Traykovski et al. (2007), whose benthic tripod data collected on the Po prodelta during winter 2002–2003 showed that gravity flows tended to occur mainly in conjunction with reasonably large waves. This approach is also consistent with the conclusions of Scully et al. (2003), who found that for the Eel shelf, realistic deposition by modeled gravity flows only occurred if the energetic wave events creating them occurred within a week or so of major flooding. The logical explanation was that initial bed consolidation over time scales of more than about a week inhibits the very rapid and massive bed resuspension needed to critically restratify the wave boundary layer. However, it should be kept in mind that wave-supported gravity flows are only one of several transport mechanisms that are capable of moving sediment away from the mouth of the Po. A significant component of the Po sediment discharged during the first half of the floood may have been transported along-shelf and away from the Po prodelta by mean currents (Nittrouer et al., 2004; Sherwood et al., 2004; Traykovski et al., 2007).

It is notable from Fig. 4 that the fall 2000 Po flood can be separated into two periods with comparable cumulative sediment discharge, each defined by a rating curve prediction of $Q_s > 2500\,\mathrm{kg\,s^{-1}}$, but with distinctly different wave activity. During the first period (cumulative $Q_s = 17$ million tons), significant wave height and peak period were only 0.38 m and 3.9 s on average. During the second half (cumulative $Q_s = 20$ million tons), mean significant height and peak period were 0.97 m and 5.0 s. Thus in applying our 2-D gravity flow model, we assume that: (i) the first (low wave) portion of the flood did not feed wave-supported gravity currents and (ii) sediment associated with the first portion of the flood was either dispersed along-shelf by mean currents or was too consolidated several weeks later to be resuspended into wave-supported gravity flows during the second (high wave) portion of the flood.

To produce realistic flood deposit thicknesses in the sub-region we modeled, we had to reduce the amount of sediment predicted by Eq. (6) by roughly 40 percent. The 20 million tons of sediment predicted by Eq. (6) for the high wave portion of the Po flood is still more than the 16 million tons observed to be associated with the fall 2000 flood layer by Wheatcroft et al. (2006) based on X-radiograph fabric or the 13 million tons observed by Palinkas et al. (2005) based on the penetration depth of ^{7}Be. There are several reasons why the coefficients used with Eq. (6) may over-predict the amount of sediment that entered into wave-supported gravity flows on the prodelta during the fall 2000 flood. First, Eq. (6) applies specifically to suspended sediment discharge before the Po separates into its distributaries. Syvitski et al. (2005) estimate that about 16% of the Po sediment load is trapped within the Po's distributary channels due to a reduction in velocity within the subsiding subaerial delta. Second, the rating curve used for Fig. 4(b) was calibrated using a comprehensive data set from the 1930s. As pointed out by Syvitski and Kettner (2007), reductions in sediment yield in the hinterland over the 20th century indicate that loads could now be 50% lower due mainly to damming of Po River tributaries. Third, our implementation of Eq. (6) does not include the random component recommended by Syvitski et al. (2005) to more realistically represent the large deviations from mean predictions which characterize the sediment loads of real rivers.

Another issue important to producing realistic deposits is the along-shelf distribution of sediment input into the gravity flows near shore. Based on observations from the 1930s and 1950s, Nelson (1970) and Syvitski et al. (2005) concluded that on average 63–74% of the Po sediment load exits the Pila and 25–35% exits the Tolle–Gnocca–Goro. Wheatcroft et al. (2006), in contrast, found only 43% of the flood deposit by mass to be in the Pila region and 57% to be off the Tolle–Gnocca–Goro (south of 44.9°N). Possible explanations for this discrepancy include southward transport by mean currents and secondary distributaries becoming more active during high discharge events (Wheatcroft et al., 2006). Two different along shelf sediment distributions were investigated here, one which spread 0.56 times the discharge predicted by (6) evenly along-shelf between 44.80 and 45.02°N during the large wave portion of the flood, and one which distributed the same total load along-shore according to a smoothed average of the along-shelf river supply inferred by Nelson (1970), Syvitski et al. (2005) and Wheatcroft et al. (2006).

3.3. 2-D model results

Fig. 5 displays the results of the 2-D model run for the high waves portion of the forcing time-series highlighted in Fig. 4. Applying 0.56 times Eq. (6) to the high wave portion of the flood and distributing the sediment load as a function of latitude according the curve on the left edge of Fig. 5 results in a total deposited mass of 11 million tons distributed in a

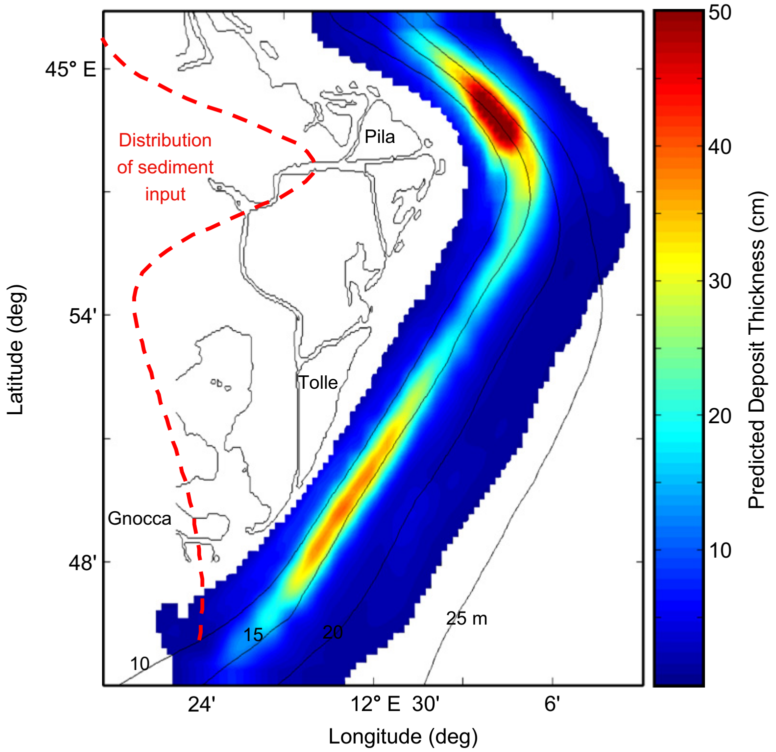

Fig. 5. Isopach map of the fall 2000 Po River flood deposit resulting from the latter, higher wave portion of the flood as indicated by the heavy arrow in Fig. 4. The sediment discharge was input as function of latitude according to the red dashed curve above, such that the total input summed to 0.56 times the instantaneous discharge curve displayed in Fig. 4. For consistency with Fig. 2, only deposits thicker than 0.5 cm and in water deeper than 5 m are shown.

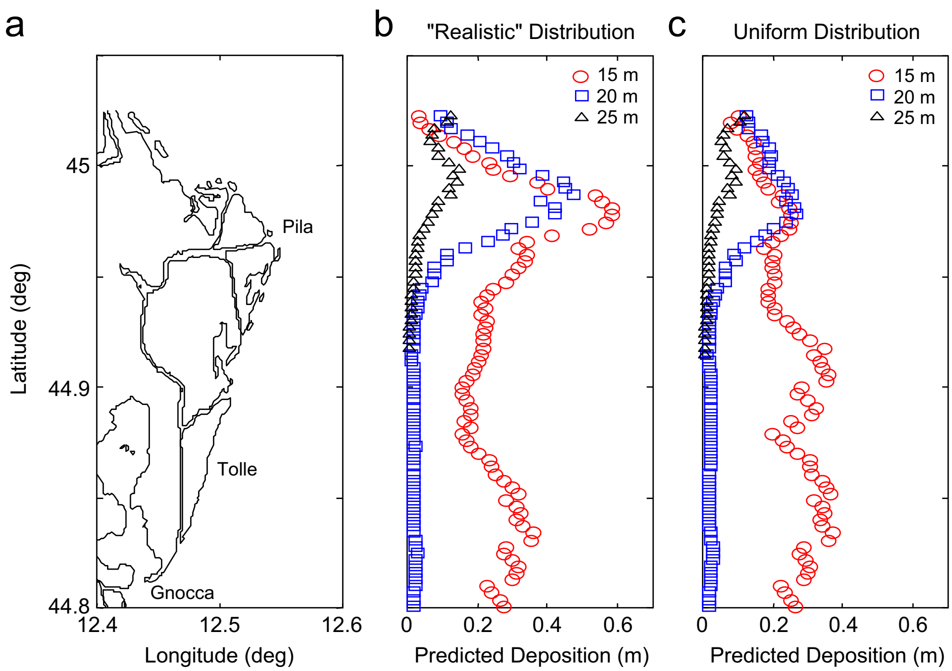

Fig. 6. Predicted flood layer thicknesses along the 15, 20 and 25 m isobaths as a function of latitude along the Po delta. (a) Location map; (b) layer thickness using the "realistic" spatially varying input distribution shown in Fig. 5; (b) layer thickness using a uniform along-shore distribution which sums to the same total sediment input. More sediment is deposited in deeper water offshore of the Pila regardless of the details of the along-shelf distribution of sediment discharge.

spatial pattern very similar to that observed by Wheatcroft et al. (2006). Note, however, that our model domain does not extend quite as far south as the observations, which further reduces the total mass of our predicted deposit. Key features common to the modeled (Fig. 5) and observed (Fig. 2) flood deposits include: (i) a total flood deposit mass which sums to between 10 and 20 million tons, (ii) two main depocenters, one off the Pila and one off the Tolle–Gnocca–Goro, (iii) thicker deposits off of the Pila than off the Tolle–Gnocca–Goro, (iv) deeper deposits off the Pila than off the Tolle–Gnocca–Goro, (v) a local tendency for deposition to occur near regions of maximum bed slope and (vi) a global tendency for along-shelf locations with greater bed slopes to exhibit thicker deposits.

Fig. 6 examines the sensitivity of the above results to the along shore distribution of sediment input by comparing the "realistic" distribution case (as in Fig. 5) with a uniform along-shelf input of sediment. Not unexpectedly, the "realistic" distribution, which inputs more sediment from the Pila, results in greater overall deposition directly off the Pila than does the uniform case. However, the influence of the along-shelf distribution of input is felt mainly in shallow water ($h \leqslant 15$ m). Along the 20 and 25-m isobaths, deposition is predicted to be significantly greater off the Pila than off the Tolle–Gnocca–Goro regardless of the relative sediment load. This insensitivity to sediment load in deeper water emphasizes the importance of bed slope in controlling deposition. All else being equal, steeper regions can move and deposit more sediment farther offshore.

Fig. 7 displays the magnitude of bed slope calculated from the model grid bathymetry. The spatial distribution of bed slope is remarkably similar to both the modeled and observed distribution of flood deposition, i.e., deposition tends to occur where bed slope reaches a maximum. This is because wave-supported gravity flows converge quickly where slope first stops increasing offshore. Only increasing slope can compensate for the decay of wave orbital velocity with depth. Otherwise sediment will converge rapidly at the depth where slope first stops increasing (see Eqs. (3)–(5)). In the next section we examine the morphodynamic implications of long-term deposition by wave-supported gravity flows responding to these local patterns in bed slope.

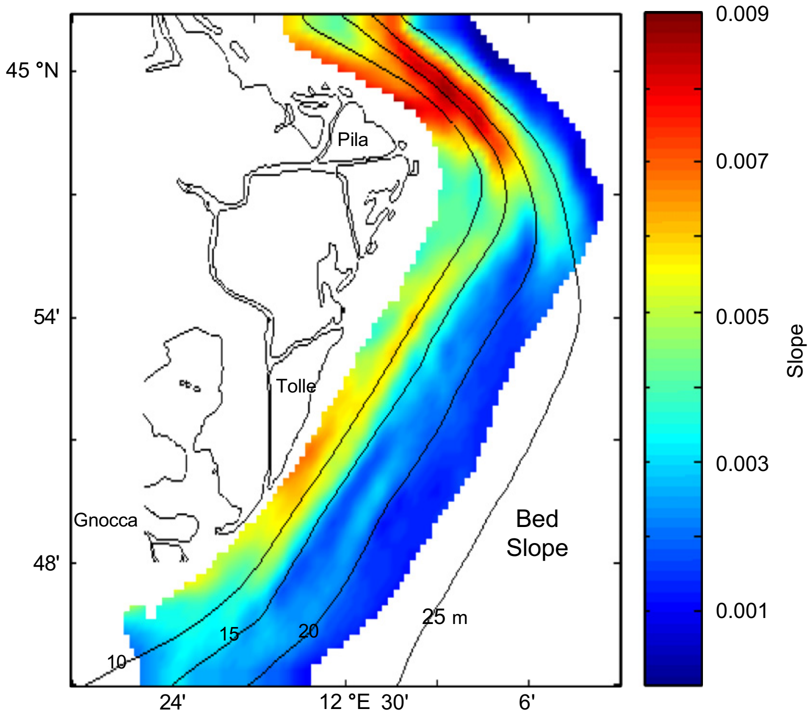

Fig. 7. Color contour plot of the absolute value of bed slope for the bathymetry shown in Fig. 1. Areas with depths less than 5 m or predicted flood deposits thinner than 0.5 cm are masked as in Fig. 5.

4. Application to century-scale evolution of the Po delta

4.1. Distinct long-term evolution of Pila vs. Tolle

The distinct bathymetries seaward of the various distributaries of the Po delta provide an ideal opportunity to test the ability of a simple wave-supported gravity flow model to account for long-term bathymetric evolution as a function of sediment supply and local subsidence. Figs. 8(a) and (b) display the evolution of bathymetry seaward of the Pila and Tolle mouths over century time-scales as documented by Nelson (1970) (based largely on data from Visentini, 1940). Present-day profiles are shown in Fig. 8(c) based on the bathymetry used to generate Fig. 1. According to Nelson, in the mid-1800s the prodelta off the Tolle was prograding seaward several times faster than the prodelta off the Pila (Figs. 8a and 8b). But in the late 1800s, the situation reversed, and for the next century the Pila prograded much faster than the Tolle. Based on the findings of Visentini (1940), Nelson (1970) reported a shoreline recession off the Tolle between 1886 and 1935 of more than a kilometer along with an associated change from a convex to a concave upward profile. The contrasting convex and concave upward profiles off the Pila and Tolle distributaries have persisted to the present day (Fig. 8c).

Nelson (1970) associated the change in progradation rates off these two distributaries with a major shift in the relative sediment discharge from these two distributaries. Before the late 1800s, the Tolle discharged several times more sediment than the Pila, whereas in the mid-20th century, the Pila typically discharged 5–10 times more sediment than the Tolle (Nelson, 1970; Syvitski et al., 2005). Between the late 1800s and the publication of the Nelson's paper, the Pila prodelta had been prograding with a stable profile shape at about 35 m yr^{-1}. According to Nelson (1970), local subsidence has also played a role in favoring bathymetric recession in the absence of high sediment discharge. Nelson suggested local subsidence on the Po prodelta to be on the order of 10 cm yr^{-1}. More recently, Carminati and Martinelli (2002) estimated maximum subsidence of the Po delta to be 6–7 cm yr^{-1}.

4.2. Long-term 1-D model implementation

To predict deposition and bathymetric evolution over time-scales of many decades, Eq. (3) was used

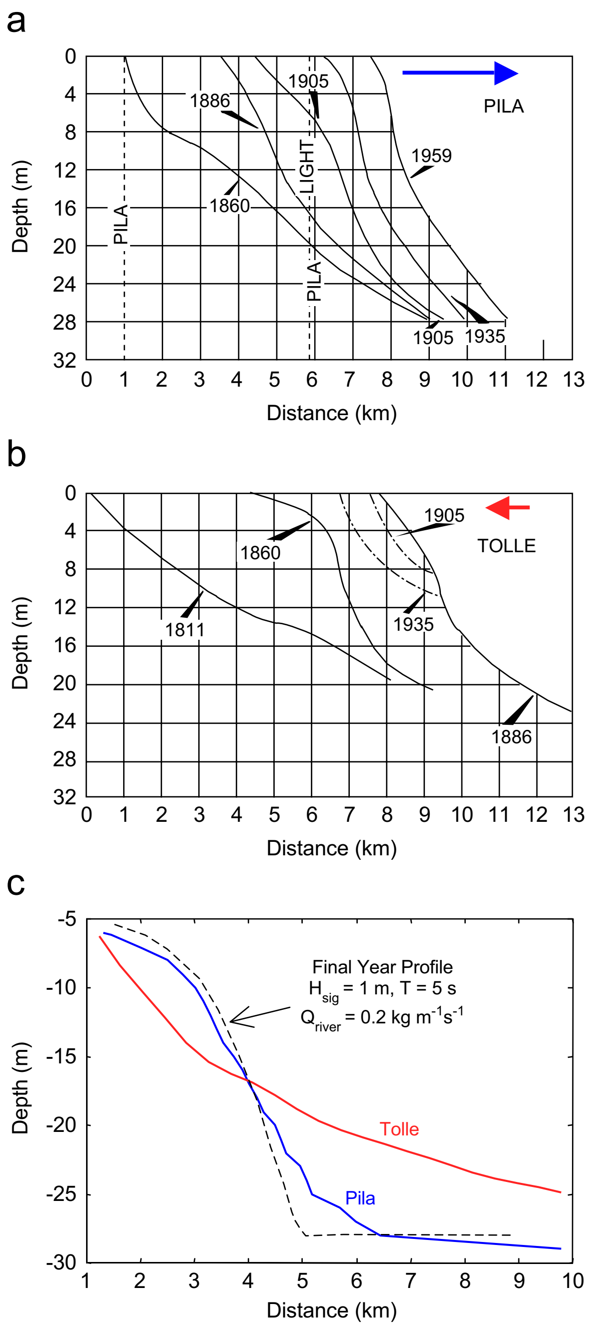

Fig. 8. Evolution of bathymetric profiles seaward of the (a) Pila and (b) Tolle mouths over century time-scales as reported in Nelson (1970). (c) Present day profiles off the Pila and Tolle as determined from the bathymetric database used for Fig. 1. Also shown in (c) is the final year profile simulation for the idealized Pila case from Fig. 9 (dashed line). Parts (a) and (b) reprinted from Nelson, B.W., Hydrography, sediment dispersal, and recent historical development of the Po River delta, Italy. SEPM Special Publication No. 15, 152–184, Copyright (1970), reproduced with permission from the Society for Sedimentary Geology.

to first calculate Q_g over a bathymetric profile with constant slope. Gradients in Q_g were then used to predict deposition, $D = -\mathrm{d}Q_g/\mathrm{d}x$, which then fed back to produce changes in bathymetry. Although temporal changes in wave height and riverine sediment supply could have been incorporated in a straightforward fashion, long-term simulations presented here kept waves and river discharge constant over the course of each seasonal flood. The across-shore grid spacing was 60 m, a 1-d time-step was used to simulate each 30-d annual flood, and bathymetry was updated after every time-step. As mentioned earlier in the context of 2-D bathymetry, the nature of the gravity-flow solution is highly sensitive to irregularities in topography. Thus, the potentially irregular deposit resulting from each time-step was run through a five-point spatial low-pass filter before updating the bathymetry.

4.3. Results of long-term modeling of subsiding delta

To investigate the long-term morphodynamic response to wave-supported gravity flows off the Pila versus the Tolle distributaries, a 140-y simulation was initiated at two contrasting sites, each consisting of a 30-d flood every year coinciding with 1-m significant wave height, 5-s waves. Each site had the same initial bathymetry (Fig. 9a and b), consisting of a linearly sloping profile extending from 2 to 28 m depth over a distance of 7 km (i.e., an initial slope of $\alpha = 0.0037$). In addition, both sites were subjected to an annual subsidence of 3 cm yr^{-1} distributed over the prodelta as shown in Fig. 9(c). The only difference between the two simulations was that the Pila-like prodelta received five times as much sediment per unit length along-shelf during the annual flood ($Q_r = 0.2\,\mathrm{kg\,m^{-1}\,s^{-1}}$) relative to the Tolle-like prodelta ($Q_r = 0.04\,\mathrm{kg\,m^{-1}\,s^{-1}}$). Consistent with the 2-D simulation in Section 3, $c_d = 0.003$ and $Ri_c = 0.25$. However, sediment porosity was set to 0.6 to represent longer-term accumulation and sediment dewatering.

Fig. 9(a) and (b) display the bathymetric changes associated with each of these simulations. Off the idealized Pila, the sediment load overwhelmed subsidence, and the profile became convex upwards as deposition proceeded. Initially, deposition was focused in shallow water, but as evolution of the profile progressed, the locus of deposition migrated to increasingly greater depths (Fig. 9a). This is because wave-supported gravity flows favor maximum deposition near the depth where slope first stops increasing with distance offshore, and the depth of maximum slope increased as the profile evolved. In contrast, off the idealized Tolle subsidence overwhelmed sedimentation near shore, causing the landward portion of the profile to recede (Fig. 9b). The prodelta steepened near shore, creating a concave-upwards profile. The depth offshore where bed slope rapidly decreases was then likewise nearer shore, and sedimentation was focused in shallower water.

Fig. 9(c) displays the cross-shore distribution of the final year of deposition for both the idealized Pila and Tolle simulations. Consistent with the pattern observed by Wheatcroft et al. (2006) and that predicted by our more realistic 2-D model of the fall 2000 flood, deposition is thicker and deeper off the Pila and thinner and shallower off the Tolle. Fig. 9(a) and (b) emphasize another difference between the two sites. Whereas the idealized Pila profile evolved to a stable form which eventually prograded seaward at a constant rate, the Tolle profile did not reach a stable form within the timeframe of the simulation. Off the Tolle, the local deposition rate shallower than about 8-m depth remained too small to counteract the imposed subsidence curve. Thus, the prodelta between 4 and 8-m depth continued to recede. In contrast, the progradation rate for the Pila-like profile became steady at about 22 m yr^{-1} during the final 80 y of the simulation.

Consistent with the observations shown in Fig. 8(a), the century time-scale, 1-D simulation of the idealized Pila in Fig. 9(a) suggests that the progradation of the prodelta off this distributary of the Po during the early 20th century may provide a case study for an equilibrium prograding clinoform moving across a shallow paleo-shelf. The "equilibrium" bathymetric profile from the final year of the idealized Pila simulation is superimposed on the modern day observed Pila bathymetry in Fig. 8(c). The reasonable correspondence suggests that the form of the bathymetric profile seaward of the Pila may still be close to equilibrium, even though the actual progradation rate has probably slowed over the last several decades in conjunction with a reduced sediment load. Given that the observed deposition off the Pila from the fall 2000

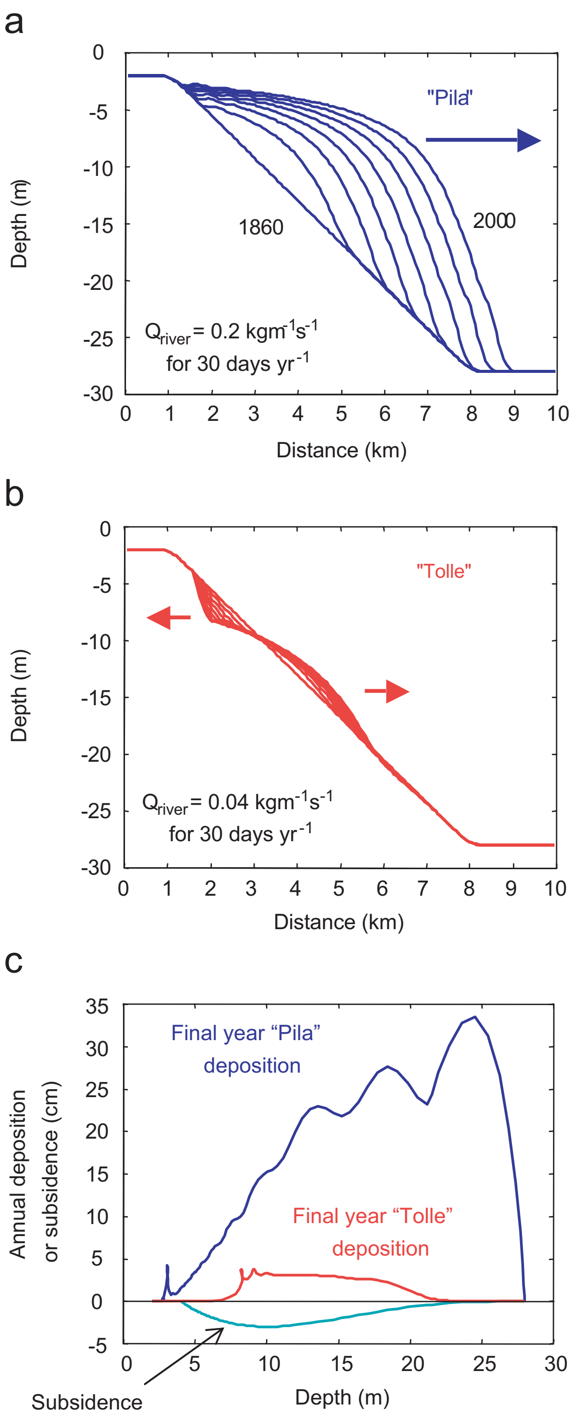

Fig. 9. Results of 140-y simulations of profile evolution associated with wave-supported gravity flows superimposed on prodelta subsidence off idealized representations of the (a) Pila and (b) Tolle distributary mouths. (c) Cross-shore distribution of the final year of deposition for both simulations along with the imposed subsidence rate. Deposition overwhelms subsidence off the Pila, leading to progradation, steepening offshore and deposition in deeper water. Subsidence overwhelms deposition off the Tolle, leading to regression, steepening near shore and deposition in shallower water.

flood is qualitatively quite similar to the "equilibrium" final year pattern in Fig. 9(c), it is possible that the large flood in the fall of 2000 may have provided a sediment load typical of smaller water discharges occurring last century when sediment yields in the hinterlands were significantly higher.

5. Discussion and conclusions

The ONR STRATAFORM project, which focused on the Eel River shelf off northern California, reignited interest in wave-supported gravity flows as a dominant mechanism for forming muddy flood deposits off high-yield rivers. Since then, wave-supported gravity flows have also been observed off the Po (Traykovski et al., 2007), and the geometry of shelves off several more rivers worldwide have been shown to be consistent with deposition by wave-supported gravity flows (Friedrichs and Wright, 2004). The aim of the present paper was to test whether wave-supported gravity flows could explain the distribution of Po flood deposits associated with the major flood of fall 2000, as well as patterns of prodelta evolution observed off the Po over the last 150 y.

Results presented here suggest that the 2-D gravity flow model applied to the Eel shelf by Scully et al. (2003) is able to reproduce key aspects of the Po 2000 flood deposit without changes in model parameterization. Consistent with the field observations (Palinkas et al., 2005; Wheatcroft et al., 2006), the 2-D model for wave-supported gravity flows produced (i) deposits in deeper water off the Pila than off the Tolle–Gnocca–Goro, (ii) a local tendency for deposition to occur near regions of maximum bed slope, and (iii) a global tendency for along-shelf locations with greater bed slopes to exhibit thicker deposits. Subject to reasonable constraints on sediment input, the model also produced an along-shelf distribution and total flood deposit mass consistent with observations.

The notable correlation of bed slope to both observed and modeled flood deposit thickness off the Po is highly consistent with the dynamics of wave-supported gravity flows. The analytical theory for such flows predicts maximum gravity-driven deposition to occur where bed slope first starts decreasing with distance offshore. This is because bed slope can counteract the tendency for wave orbital decay to reduce transport capacity only where slope increases offshore. Once bed slope stops increasing with depth, the effects of bed slope and decaying wave orbital velocity work together to drive very rapid transport convergence. Furthermore, the greater the bed slope is when it starts decreasing, the greater the convergence rate will be at that point. Thus along-shelf locations with greater maximum bed slope tend to exhibit thicker deposits (as long as bed slope is not so great that it triggers auto-suspending turbidity currents).

The modeled flood deposit had a thickness and total mass in general agreement with observations (Palinkas et al., 2005; Wheatcroft et al., 2006) assuming (i) gravity flows were restricted to the more energetic second half of the fall 2000 flood, and (ii) riverine sediment input was reduced to ~60% of the rating curve originally calibrated with observations from the 1930s (Syvitski et al., 2005). Modeling results were further improved by distributing riverine sediment supply along-shelf according to a smoothed spatial average of the relative distributary discharges suggested by others (Nelson, 1970; Syvitski et al., 2005; Wheatcroft et al., 2006). Gravity-driven deposition in "deep" water (depth > 15 m) was much less sensitive to the along-shelf distribution of riverine input than was deposition in shallower water. In deeper water, the reduced carrying capacity associated with wave orbital decay means that orbital velocity in concert with bed slope is more likely to limit transport and deposition.

The latter portion of this paper marks the first time the gravity flow formulation of Wright et al. (2001) has been used to predict deposition over time-scales long enough to change shelf bathymetry and thus feedback to alter the location of further gravity-driven deposition. The distinct bathymetries seaward of the various distributaries of the Po delta provided an excellent opportunity to test the ability of the wave-supported gravity flow model to account for long-term bathymetric evolution as a function of sediment supply and local subsidence. A 140-y simulation was initiated for idealized representations of the bathymetry offshore of the Pila and Tolle, with each site subjected to subsidence on the order of that observed off the Po. The only difference between the two simulations was that the Pila-like prodelta received five times as much sediment per unit length along-shelf during each annual flood, consistent with historical rating curves for each distributary (Syvitski et al., 2005).

Sediment supply overwhelmed subsidence off the idealized Pila, and the profile quickly evolved to an equilibrium prograding clinoform as deposition proceeded. In contrast, subsidence overwhelmed deposition off the Tolle, causing the landward part of the profile to recede, and the prodelta off the Tolle did not reach a stable form within the duration of the simulation. Over the course of the simulation, the locus of deposition offshore of each distributary remained near the depth where the bed slope first stopped increasing with distance offshore, consistent with basic control of bathymetry on deposition by wave-supported gravity flows.

Together, the short- and long-term simulations presented in this paper highlight the three fundamental controls on deposition by wave-supported gravity currents: sediment supply, waves and bathymetry. For such deposition to occur at all, fine sediment supply must be sufficient to overwhelm the capacity of the wave boundary layer. Thus, deposition tends to occur where and when sediment supply is concentrated, i.e., relatively close to river mouths and mainly during river floods. The second necessary ingredient, namely waves, further constrains when deposition by wave-supported gravity flows occurs and also creates the characteristic gap between the shoreline and the locus of deposition. Very close to shore, the large magnitude of wave orbital velocity can transport most of the sediment offshore, but in deeper water, the decayed near-bed orbital velocity has a much smaller capacity. Finally, existing bathymetry dictates the depth at which changes in bed slope will focus sediment transport convergence—typically where bed slope first stops increasing offshore.

There are several aspects of gravity-driven deposition off high-yield rivers which are ripe for further study. For example, this paper used forward modeling to show that wave-supported gravity flows can lead to seaward progradation of stable, "equilibrium" profiles. To more clearly highlight the controlling parameters, a next logical step would be to solve analytically, without time-stepping, for the shape of equilibrium prograding clinoforms formed by wave-supported gravity flows as a function of sediment supply, wave properties and changes in base level. Although recent work has highlighted the diverse geographic relevance of wave-supported gravity flows, there are important cases where tides or wind-driven currents suspend gravity flows off of high yield rivers. Recent work (Walsh et al., 2003) suggests that prodeltas/clinoforms dominated by tides are significantly broader than those dominated by waves, for example.

Acknowledgments

Funding was provided by the Office of Naval Research Coastal Geosciences Program (Grants N00014-03-10144 and N00014-04-10628) as part of the EuroSTRATAFORM Program and by the National Science Foundation Marine Geology and Geophysics Program (Grant OCE-0326831). A. Kettner and J. Syvitski generously provided sediment discharge rating curve coefficients for the Po River. Wave data were kindly provided by L. Cavaleri. Bathymetric data from Correggiari et al. (2001) were shared generously by F. Trincardi. Helpful comments were provided by A. Cattaneo, C. Nittrouer, C. Paola and R. Wheatcroft. This paper is Contribution No. 2689 of the Virginia Institute of Marine Science, The College of William and Mary.

References

Carminati, E., Martinelli, G., 2002. Subsidence rates in the Po Plain, northern Italy: the relative impact of natural and anthropogenic causation. Engineering Geology 66, 241–255.

Correggiari A., Cattaneo, A., Trincardi, F., 2005. Depositional patterns in the Late-Holocene Po delta system. In: Bhattacharya, J.P., Giosan, L. (Eds.), River Deltas: Concepts, Models and Examples. SEPM Special Publication 83 365–392.

Correggiari, A., Trincardi, F., Langone, L., Roveri, M., 2001. Styles of failure in Late Holocene high stand prodelta wedges on the Adriatic shelf. Journal of Sedimentary Research 71, 218–236.

Fox, J.M., Hill, P.S., Milligan, T.G., Boldrin, A., 2004. Flocculation and sedimentation on the Po River Delta. Marine Geology 203, 95–107.

Friedrichs, C.T., Wright, L.D., 2004. Gravity-driven sediment transport on the continental shelf: implications for equilibrium profiles near river mouths. Coastal Engineering 51, 795–811.

Moore, D.G., 1969. Reflection profiling studies of the California Continental Borderland: structure and quaternary turbidite basins. Geological Society of America, Special Paper no. 107, 142p.

Nelson, B.W., 1970. Hydrography, sediment dispersal, and recent historical development of the Po River delta, Italy. SEPM Special Publication no. 15, pp. 152–184.

Nittrouer, C.A., Miserocchi, S., Trincardi, F., 2004. The PASTA project: investigation of Po and Apennine sediment transport and accumulation. Oceanography 17 (4), 46–57.

Ogston, A.S., Cacchione, D.A., Sternberg, R.W., Kineke, G.C., 2000. Observations of storm and river flood-driven sediment transport on the northern California continental shelf. Continental Shelf Research 20, 2141–2162.

Palinkas, C.M., Nittrouer, C.A., Wheatcroft, R.A., Langone, L., 2005. The use of ^{7}Be to identify event and seasonal sedimentation near the Po River delta, Adriatic Sea. Marine Geology 222–223, 95–112.

Pirmez, C., Pratson, L.F., Steckler, M.S., 1998. Clinoform development by advection–diffusion of suspended sediment: modeling and comparison to natural systems. Journal of Geophysical Research 103, 24,141–24,157.

Puig, P., Ogston, A.S., Mullenbach, B.L., Nittrouer, C.A., Sternberg, R.W., 2003. Shelf-to-canyon sediment-transport processes on the Eel continental margin (northern California). Marine Geology 193, 129–149.

Scully, M.E., Friedrichs, C.T., Wright, L.D., 2002. Application of an analytical model of critically stratified gravity-driven sediment transport and deposition to observations from the Eel River continental shelf, northern California. Continental Shelf Research 22, 1951–1974.

Scully, M.E., Friedrichs, C.T., Wright, L.D., 2003. Numerical modeling results of gravity-driven sediment transport and deposition on an energetic continental shelf: Eel River, northern California. Journal of Geophysical Research 108 (C4), 171–1714.

Sherwood, C.R., Carniel, S., Cavaleri, L., Chiggato, J., Das, H., Doyle, J.D., Harris, C.K., Niedoroda, A.W., Pullen, J., Reed, C.W., Russo, A., Sclavo, M., Signell, R.P., Traykovski, P., Warner, J.C., 2004. Sediment dynamics in the Adriatic Sea investigated with coupled models. Oceanography 17 (4), 118–131.

Swenson, J.B., Paola, C., Pratson, L., Voller, V.R., Murray, A.B., 2005. Fluvial and marine controls on combined subaerial and subaqueous delta progradation: morphodynamic modeling of compound-clinoform development. Journal of Geophysical Research 110, F02013.

Syvitski, J.P.M., Kettner, A.J., 2007. On the flux of water and sediment into the northern Adriatic Sea. Continental Shelf Research 27, 296–308.

Syvitski, J.P.M., Kettner, A.J., Correggiari, A., Nelson, B.W., 2005. Distributary channels and their impact on sediment dispersal. Marine Geology 222–223, 75–94.

Traykovski, P., Geyer, W.R., Irish, J.D., Lynch, J.F., 2000. The role of wave-induced density-driven fluid mud flows for cross-shelf transport on the Eel River continental shelf. Continental Shelf Research 20, 2113–2140.

Traykovski, P., Wiberg, P.L., Geyer, W.R., 2007. Observations and modeling of wave-supported sediment gravity flows on the Po prodelta and comparison to prior observations from the Eel shelf. Continental Shelf Research 27, 375–399.

Visentini, M., 1940. Ricerche idrografiche nel Delta del Po: 1st. Poligrafico Stato (Roma), Ufficio Idrographico Po-Parma, Pub. 14, v. 2, 175 p., 18 pls.

Walsh, J.P., Driscoll, N.W., Nittrouer, C.A., 2003. Marine dispersal of fine-grained river sediment: environmental controls on subaqueous-delta clinoforms. Geological Society of America Abstracts with Programs 35 (6), 625.

Wheatcroft, R.A., Stevens, A., Hunt, L.M., Lewis, R., 2006. The large-scale distribution and internal geometry of the fall 2000 Po River flood deposit: evidence from digital x-radiography. Continental Shelf Research 26, 499–516.

Wright, L.D., Friedrichs, C.T., Kim, S.C., Scully, M.E., 2001. The effects of ambient currents and waves on the behavior of turbid hyperpycnal plumes on continental shelves. Marine Geology 175, 25–45.